Atomistic Simulation of Nafion Membrane: I. Effect of Hydration on Membrane Nanostructure

R. Devanathan,* A. Venkatnathan, and M. Dupuis

Fundamental Science Directorate, Pacific Northwest National Laboratory, Richland, Washington 99352

Received: April 5, 2007

We used classical molecular dynamics simulation with the DREIDING force field to characterize the changes in the nanostructure of Nafion membrane brought about by systematically changing the hydration level. We calculated the relative percentages of free, weakly bound, and bound water in hydrated Nafion membranes. At low hydration levels, coordination of hydronium ions by multiple sulfonate groups prevents vehicular transport and impedes structural transport of protons through steric hindrance to hydration of the hydronium ions. Our results provide insights into the nanostructure of hydrated Nafion membrane and are in excellent agreement with experimental observations by neutron scattering of changes in the percentage of non diffusing hydrogen atoms.

1. Introduction

Polymer electrolyte membrane (PEM) fuel cells represent the critical step in the hydrogen economy, which has been proposed as an alternative to the current fossil fuel-based economy and its associated problems of unreliable energy supply, environmental pollution, and greenhouse gas emission.[1] PEM fuel cells convert the chemical energy of the fuel (hydrogen or other fuel like methanol) into electrical energy with high efficiency and minimal pollution. They have potential applications in the areas of transportation, distributed power, and portable power for electronic devices. Widespread commercialization of this promising technology has been hampered by high production cost and the need for improvements in performance, durability and service life of fuel cells under a variety of operating conditions.

The heart of the PEM fuel cell is a polymer membrane that separates the reactant gases and conducts protons.[2] Perfluorosulfonic acid (PFSA)-based membranes, such as Nafion developed by DuPont, are the most widely used in PEM fuel cells. Despite advances in the development of alternative membranes, Nafion is considered the benchmark, because it has been by far the most extensively studied.[3] The structure and properties of Nafion[3] and other proton exchange membranes[4] have been reviewed recently. None of the available membranes meets the requirements of high proton conductivity, impermeability to gases, low electro-osmotic drag to avoid water and methanol (in direct methanol fuel cell) transport, good mechanical and chemical stability under a range of temperatures and hydration levels, and low cost.

In Nafion, a hydrophobic CF_2 backbone and a highly hydrophilic sulfonic acid-terminated pendant are known to form nanoscale domains within which ionic transport occurs.[3,5−6] The dissociation of SO_3H groups and subsequent proton transport in Nafion depends on the presence of liquid water, which restricts the operating temperature to below 100 °C at ambient pressure. However, operation at higher temperatures offers the potential to enhance the kinetics of the electrochemical reactions at the electrodes and reduce the susceptibility of catalysts to CO poisoning. These opposing requirements call for the development of novel membranes based on a sound molecular-level understanding of the nanostructure of existing membranes, such as Nafion, and its influence on transport properties and membrane performance.

Mauritz and Moore[3] have reviewed the extensive experimental database on the morphology of Nafion membranes. Experimental studies have used a variety of X-ray and neutron scattering and diffraction techniques, electron microscopy and atomic force microscopy, and spectroscopic techniques to characterize the molecular structure of hydrated PFSA membranes. Due to the inability of experiments to directly observe the structure and dynamics of the membrane under different levels of hydration, there is no universally accepted model of the structure of Nafion. The general consensus[3] appears to favor a connected nanoscale network of ionic domains that are anisotropic in shape and heterogeneous in spatial distribution, and through which ionic transport takes place. The water present in the membrane is considered to exist in different states, such as strongly bound to the sulfonate group, weakly bound, and free. While the small time and distance scales associated with molecular transport through these ionic domains limit experimental observation, they are well suited for study by atomistic simulation.

Modeling and simulation studies of PFSA membranes have included ab initio calculations of the role of side chains of Nafion in effecting proton transfer,[7−8] molecular dynamics (MD) simulations of hydrated Nafion,[9−18] mesoscale modeling of the morphology of the hydrated membrane,[19] and statistical mechanical modeling of Nafion pores.[20] All of this work reflects the multiscale nature of transport processes in polymer membranes. At the most fundamental level, proton-transfer processes have to be modeled quantum mechanically. Proton transport involves both structural diffusion (migration of a topological defect in a hydrogen-bonded network) and vehicular diffusion of hydronium ions.[21] The former has to be modeled using computationally intensive ab initio methods (see the recent review by Marx[21] and references therein), while the latter can be studied using classical MD with empirical force fields. Classical MD is also well suited to the size and time scale of water and small molecule transport. Much longer scale simula-

* Corresponding author. E-mail: ram.devanathan@pnl.gov.

10.1021/jp0726992 CCC: $37.00 © 2007 American Chemical Society
Published on Web 06/20/2007

tions are needed to model dynamical changes in the membrane morphology and gain insights into performance degradation upon prolonged operation.

Paddison and Elliott[8] have concluded from their ab initio modeling of PFSA side chains that proton transfer to water is possible at a hydration of less than three water molecules per sulfonate when two sulfonate groups are present close to each other in contrast to the three water molecules needed when sulfonate groups are far apart. Their study also shows hydrated protons bridging the sulfonate groups at low levels of hydration. The level of hydration is typically represented by λ, the total number of water molecules and hydronium ions per sulfonate group. It is useful to describe the hydration in terms of λ, because the sulfonate group plays a crucial role in proton transport and the weight percent of water can vary if the lengths of the backbone and side chain are changed. Elliott et al.[9] used classical MD with a modified DREIDING[22] force field to study the dynamics of small molecules in a model Nafion membrane for $\lambda \sim 1$, 3.8, and 9.7. They observed water segregation into bound water associated with the sulfonate group and more loosely attached free water. Vishnyakov and Neimark[10] used a simplified united-atom force field in their MD simulation of hydrated Nafion with K^+ counterions for three different λ values. The highest λ simulated was ~8.7. They found that as the water content increased, water clusters formed dynamically and broke apart resulting in temporary bridges between clusters instead of permanent water channels. Urata et al.[11] have also used a similar united-atom force field to model hydrated Nafion for $\lambda \sim 2.8$, 5.9, 13.3, and 35.4. They observed that at low λ, the sulfonate groups aggregated and shared water molecules, while at high λ, frequent exchange occurred between bound and free water molecules. United-atom force fields have the advantage that a larger system can be simulated compared to all-atom force fields. For instance, Urata et al.[11] have simulated systems containing 11904−24299 particles for 1.3−2.5 ns. The all-atom approach is more rigorous and computationally intensive, but is required to establish benchmarks that can validate subsequent coarse-grained simulations.

Jang et al.[12] have used an all-atom approach in their MD simulation of nanophase segregation and transport in Nafion for $\lambda = 16$. Their simulation employed a recently modified version of the DREIDING[12,22,23] force field for Nafion and the F3C[24] force field for water. This study did not bias the simulation by imposing any particular geometry for water distribution in the membrane. The authors found water transport to be strongly dependent on membrane nanostructure and calculated water diffusion coefficients at 300 and 353 K in good agreement with experimental values. In addition, recent all-atom MD simulations of hydrated Nafion[13−15] show that the interaction of the hydronium ions with the sulfonate groups of the pendant plays an important role in the diffusion of water molecules and vehicular transport of hydronium ions.

In order to study structural transport in addition to vehicular transport, Spohr[16] has incorporated non-classical proton dynamics into MD simulations of a simple slab model of a Nafion pore using a two-state empirical valence-bond (EVB) model. This study shows that structural diffusion is an important part of proton transport in MD simulations and that proton transport decreases with decreasing λ due to the formation of the $H_5O_2^+-SO_3^-$ ion-pair. Spohr[16] has pointed out the need for studying large systems with several realistic pores. Petersen et al.[17,18] have used a self-consistent multistate EVB method to characterize solvation and transport of hydrated protons in Nafion. They found that the structural and vehicular components of proton diffusion in Nafion were of similar magnitude but strongly negatively correlated. This resulted in the total diffusion of protons being comparable to its vehicular component. This is in contrast to the situation in bulk water where structural diffusion accounts for nearly 70% of the total diffusion and there is no negative correlation of structural and vehicular components.[18] While these studies have focused on a realistic treatment of proton transport and local structure around the sulfonate group, Wescott et al.[19] have examined the membrane morphology using self-consistent mean field theory with parameters derived from atomistic simulation. They observed irregularly shaped water clusters of 2−5 nm size that formed a percolated network at $\lambda = 16$. Paul and Paddison[20] have used a statistical mechanical model to study proton transport in PFSA membranes. Their study shows that much of the proton transport occurs in the center of a model pore away from the sulfonate groups. Paul and Paddison[20] have pointed to the need for further modeling to understand proton transport in polymer membranes.

Pivovar and Pivovar[25] have used quasielastic neutron scattering to study the dynamic behavior of water in Nafion as a function of λ from 1 to 16. Their work shows that a transition in membrane morphology occurs around $\lambda = 7$. The radius of a confining sphere within which water diffusion was assumed to occur increased with increasing λ and attained saturation around $\lambda = 7$. The fraction of nondiffusing hydrogen decreases with increasing λ and levels off around $\lambda = 7$. All the extracted parameters showed rapid change with λ at low hydration and asymptotic behavior at high hydration. Similar observations have been made by Moilanen et al.[26] using infrared spectroscopy to study water in Nafion for λ from 1 to 9. Their findings indicate that an abrupt structural change occurs in the membrane around $\lambda = 5$, which dramatically reduces the number of bound water molecules. However, the nature of the structural change is not understood. The studies discussed above have demonstrated the importance of systematically varying the level of hydration and studying the membrane nanostructure, especially around the sulfonate groups, using atomistic simulations.

In the present work, we have used all-atom MD simulations to systematically examine eight different levels of membrane hydration ($\lambda = 1$, 3, 5, 7, 9, 11, 13.5, and 20) to closely mirror the experimental studies of Pivovar and Pivovar[25] and Moilanen et al.[26] We have also simulated bulk water to develop a novel criterion to identify free water in Nafion. This has enabled the quantification of the fraction of free, weakly bound and bound water molecules as a function of λ. This paper, the first in a two part series, focuses on changes in the nanostructure of the Nafion membrane with systematic changes in hydration. The corresponding changes in the transport of water and hydronium ions will be discussed in the second paper. Our results establish classical benchmarks for hydrated Nafion, provide insights into experimentally observed changes in Nafion with hydration[25,26] and are in good accord with experiments.

The paper is organized as follows: in section 2, we give the details of the simulations; in section 3, we discuss the interactions of hydronium ions and water molecules with the sulfonate group, hydration of the side chain and backbone and the relative proportions of bound, weakly bound and free water; in section 4, we summarize our findings.

2. Details of the Simulation

We performed classical molecular dynamics simulations of Nafion, water, and hydronium ions using all-atom (as opposed to united atom) force fields. The chemical structure of the Nafion chain simulated in the present work is shown in Figure 1. Our

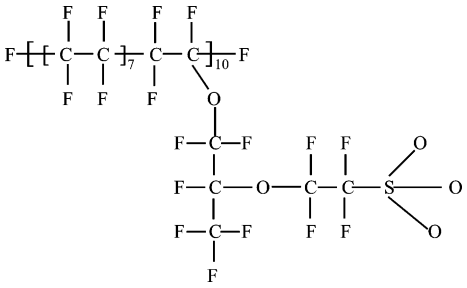

Figure 1. Chemical structure of Nafion.

TABLE 1: Weight Percentage of Water, Simulated Density, and Experimental Density[28] of Hydrated Nafion as a Function of λ

λ	H_2O wt. %	ρ_{sim} (g/cm^3)	ρ_{exp}[28] (g/cm^3)
1	1.54	1.76	2.02
3	4.50	1.80	1.96
5	7.28	1.82	1.90
7	9.90	1.78	1.86
9	12.38	1.76	1.81
11	14.72	1.76	1.78
13.5	17.48	1.68	1.73
20	23.89	1.62	1.64

TABLE 2: Average Percentage of Undercoordinated Water Molecules in Bulk Water for Various Nearest Neighbor Cutoff Distances (r_{nn})

r_{nn} (Å)	% under-coordinated
3.3	15.28
3.4	7.73
3.5	3.59
3.6	1.54
3.7	0.58
3.8	0.20
3.9	0.07
4.0	0.02

simulation cell contained four chains of Nafion (40 SO_3^-) with hydrophilic SO_3^--terminated pendants spaced evenly by seven nonpolar $-CF_2-CF_2-$ monomers (N) that form a hydrophobic backbone, referred to as a dispersed sequence by Jang et al.[12] We assume all the sulfonate groups to be ionized based on the findings of Paddison and Elliott[8] for $\lambda \geq 3$. We simulated the case of $\lambda = 1$ merely to establish a classical benchmark while being aware of the limitations of the classical hydronium ion model for this particular hydration level in light of ab initio calculations[8] that indicate that the proton is unlikely to transfer from the sulfonic acid group to water at $\lambda = 1$. In the extended chain configuration, adjacent SO_3^- groups are separated by more than 20 Å. We generated four Nafion chains of 682 atoms each by linking the polar monomeric unit (P) to the end of the nonpolar monomeric unit N_7, repeating the procedure nine times to obtain $(N_7P)_{10}$, in the notation of Jang et al.,[12] and terminating the two ends with F. To ensure charge neutrality, we added a total of forty H_3O^+ ions and solvated the membrane by adding water molecules corresponding to a given λ. As in the simulation of Jang et al.,[12] we have not biased our simulation by imposing a particular geometrical distribution of water molecules nor any predetermined density.

We minimized the energy of each model containing four Nafion chains, 40 H_3O^+ ions and 0−760 H_2O molecules separately using the steepest descent algorithm.[27] We annealed the final structure obtained from the minimization procedure in four steps as follows: (1) NPT MD simulation for 100 ps at 300 K; (2) NVT MD simulation for 50 ps with the temperature raised from 300 to 600 K; (3) NVT MD simulation for 50 ps at 600 K; and (4) NVT MD simulation for 50 ps with the temperature lowered from 600 to 300 K. We repeated this four step process three times and used the final structure as the starting configuration for a NPT MD equilibration for 250 ps at 300 K to attain the final density. This density is listed in Table 1 along with the weight percent of water in the membrane and the experimental density for the eight different values of λ examined. The experimental density reported here for membrane equivalent weight of 1148 amu is based on a fit to experiment by Morris and Sun[28] given by

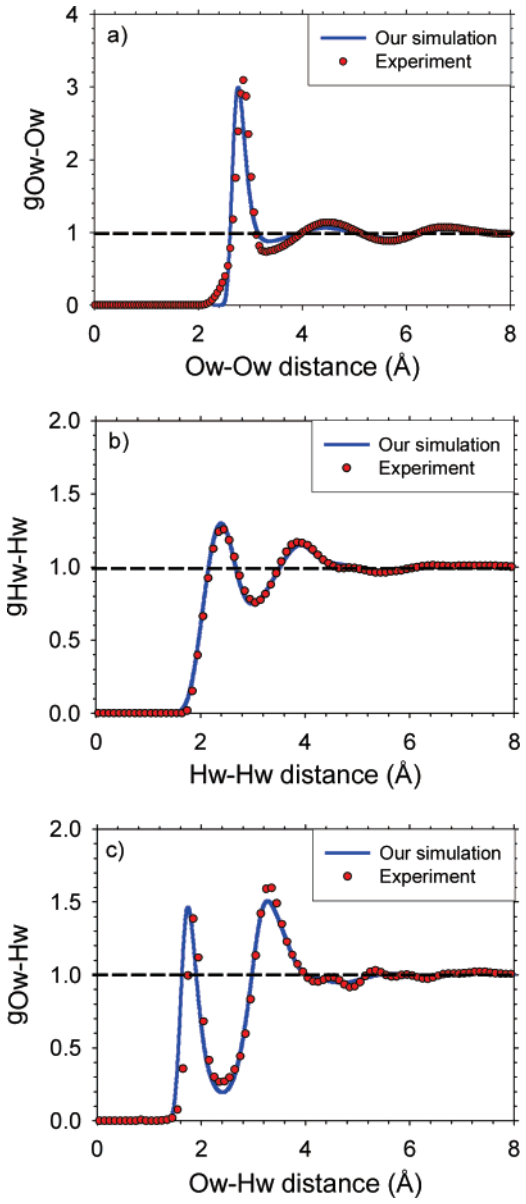

Figure 2. Radial distribution functions of (a) oxygen−oxygen, (b) hydrogen−hydrogen, and (c) oxygen−hydrogen pairs in bulk water from the present simulation (line) and experiment[32] (dots).

$$\rho\left(\frac{g}{cm^3}\right) = \frac{63.7 + \lambda}{31.1 + \lambda} \quad (1)$$

The agreement with experiment is within 5% for λ above 3, while the simulated values at $\lambda = 1$ and 3 deviate from experimental values by about 13 and 8%, respectively. We performed 2 ns NVT MD simulations at 300 K for each λ and saved the configurations every 0.2 ps (10000 configurations)

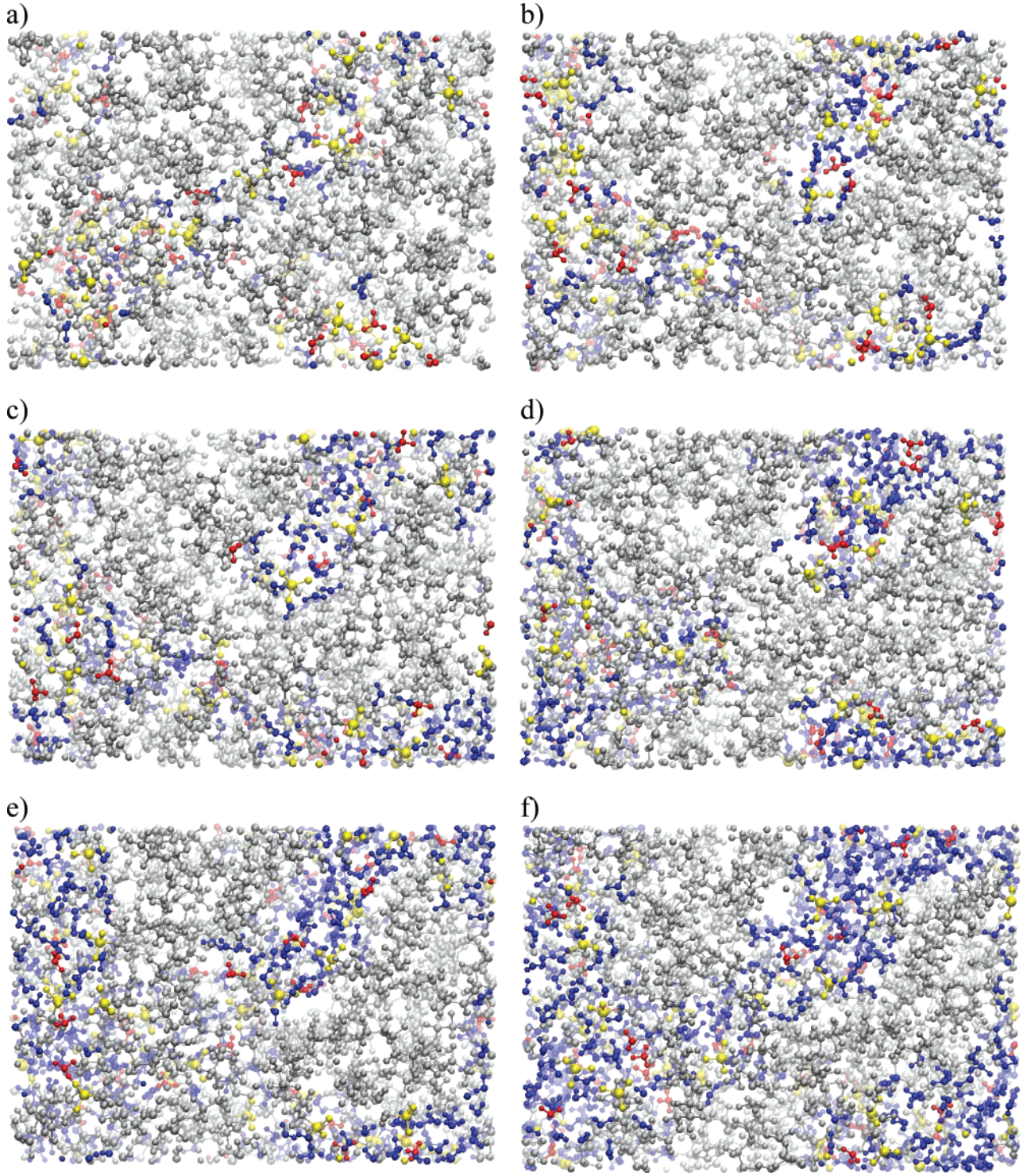

Figure 3. Orthographic projection (~42 Å × 30 Å) of hydrated Nafion for the following λ values: (a) 3; (b) 5; (c) 7; (d) 9; (e) 11; and (f) 13.5. Water molecules, hydronium ions, sulfonate groups, and the rest of the membrane are represented in blue, red, yellow, and gray, respectively.

for subsequent analysis of structural and dynamical properties. The step size for the integration was 1 fs.

We used the DL_POLY 2.16 code[29] to perform our MD simulation with the DREIDING force field[22] including recent modifications to the fluorocarbon part[23] to describe the Nafion membrane and the F3C force field[24] to describe water molecules. The flexible three-center model for water (F3C)[24] is specifically designed for use in MD simulations of macromolecules. In this model, the water molecules have flexible bond lengths and bond angles and the interaction centers are located on the three atoms. The functional forms, partial charges, and parameters of these potentials for Nafion, water and hydronium ions have been described in detail elsewhere[12,22−24] and we will not present them here. Due to a typographic error, the unit of the force constant for the angle bending term in the DREIDING potential has been incorrectly specified previously[12] as kcal mol^{-1} deg^{-2} instead of kcal mol^{-1} rad^{-2}. Following the work of Vishnyakov and Neimark,[30] we have neglected the FCCF and FCCC dihedrals in the Nafion backbone to reduce computational intensity. We used the smooth particle mesh Ewald method[31] to calculate electrostatic interactions with a cut off distance of 8 Å and a tolerance factor, also known as Ewald sum precision, of 10^{-6}.

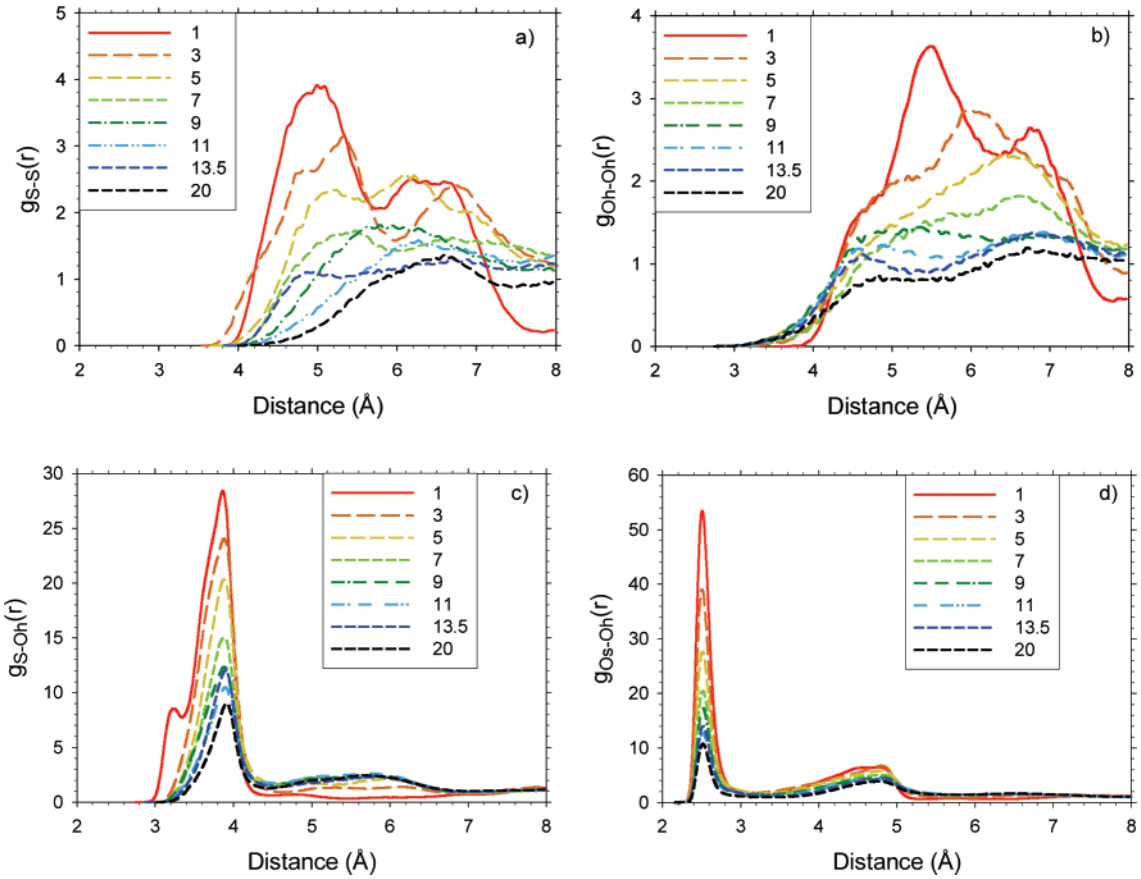

Figure 4. Radial distribution functions at various hydration levels (λ indicated by the legend) of (a) sulfur−sulfur, (b) hydronium oxygen−hydronium oxygen, (c) sulfur−hydronium oxygen, and (d) sulfonate oxygen-hydronium oxygen pairs.

In an effort to establish a criterion for identifying free water molecules in hydrated Nafion, we have also simulated a bulk water system at 300 K with 1000 F3C[24] water molecules by starting with a cubic box at the experimental density, performing 250 ps NPT MD annealing at 300 K, and then calculating properties over 2 ns using NVT MD simulations with an integration time step of 1 fs. The simulated density was 1.00 g/cm^3 at 300 K. Figure 2 shows our calculated radial distribution function (RDF) of oxygen−oxygen (O_w-O_w), oxygen−hydrogen (O_w-H_w), and hydrogen−hydrogen (H_w-H_w) pairs in bulk water represented by a line and the corresponding experimental values of Soper and Phillips[32] represented by dots. The RDF, $g(r)$, is the ratio of the local number density of an interacting molecular pair at a distance r to the average number density of the pair in the simulation cell. The agreement between our simulation and experiment is excellent. We examined the O_w-O_w coordination number (CN) of oxygen atoms in bulk water as a function of cut off distance for defining a first neighbor. Table 2 lists the percentage of undercoordinated water molecules (CN < 4) calculated from 100 configurations (10 ps apart) each containing 1000 water molecules. We find that for a first neighbor cutoff distance (r_{nn}) based on the RDF of Figure 2 (3.3 Å), about 15.3% of water molecules are undercoordinated and this figure drops to 0.02% for $r_{nn} = 4$ Å. On the basis of this data, we define a free water molecule in Nafion as any water molecule whose oxygen atom (O_w) is surrounded by four other oxygen atoms within a distance of 4 Å.

3. Results and Discussion

3.1. Distribution of Water Molecules and Hydronium Ions. Figure 3 shows an orthographic projection of the hydrated Nafion simulation box at the end of the 2 ns MD simulation visualized using the software VMD.[33] The simulation cell is periodically repeated. The size of the projection varies from 41.1 × 28.7 Å for a hydration level of $\lambda = 3$ (a) to 44.3 × 30.9 Å for $\lambda = 13.5$ (f). Depth is indicated by showing the atoms closer to the top in a darker shade of blue, red, yellow, and gray, respectively, for water molecules, hydronium ions, sulfonate groups, and the rest of the membrane. At $\lambda = 3$, hydronium bridges between sulfonate groups are seen, for instance, at the bottom right of Figure 3a. Water molecules and hydronium ions are found close to the sulfonate groups. With increasing level of membrane hydration, water molecules are more likely to be found away from the sulfonate groups and form a network of increasing spatial extent. The water domains do not appear to conform to simple shapes, such as spherical clusters, although larger scale simulations are probably needed to address this issue. Moreover, with increasing λ, water molecules mediate the interaction between hydronium ions and the sulfonate groups of the pendant. These observations are consistent with the ab initio calculations of Paddison and Elliott.[8]

3.2. Sulfonate Group−Hydronium Ion Interaction. Quantitative information about molecular interactions in hydrated Nafion is available from the RDF. Figure 4 shows $g(r)$ corresponding to the interactions of sulfur (S), sulfonate oxygen (Os) and hydronium oxygen (Oh) for various levels of hydration from $\lambda = 1$ to 20. This data was obtained from 10000 configurations at 0.2 ps intervals. The trends in our $g_{S-S}(r)$ plot in Figure 4a agree well with the work of Jang et al.[12] for λ =16. Our results also show general agreement with the trends in $g_{S-S}(r)$ computed using a different all-atom force field.[15] The first peak in Figure 4a shifts from 5.0 Å at $\lambda = 1$, through 5.3

TABLE 3: The Average Coordination Numbers of Hydronium Ions around Sulfur (n_{sh}) and Water Molecules around Sulfur (n_{sw}) in Nafion as a Function of λ

λ	n_{sh}	n_{sw}
1	2.46	0.00
3	2.05	2.23
5	1.59	3.65
7	1.14	4.26
9	0.97	4.81
11	0.77	5.34
13.5	0.76	5.33
20	0.49	5.79

Å at $\lambda = 3$, to 6.7 Å at $\lambda = 13.5$ and 20. The position of the first peak in our $g_{S-S}(r)$ differs from that in united-atom simulations.[11,14] Cui et al.[14] observed a sharp first peak at ~4 Å at all hydration levels and nonmonotonic trends in $g_{S-S}(r)$ with increasing membrane hydration. In contrast, Urata et al.[11] observed the first peak shifting from ~5 Å at $\lambda = 2.8$ to ~6 Å at $\lambda = 35.4$ and the peak becoming shorter and broader with increasing hydration. This is consistent with our finding that with increasing λ, the average S−S coordination number at a given distance decreases. The average distance from a sulfur atom within which another sulfur atom can be found (coordination number $n_{S-S}(r) = 1$) is 5.3, 5.6, 6.0, 6.5, 6.6, 7.0, 7.1, and 7.9 Å, respectively, at $\lambda = 1$, 3, 5, 7, 9, 11, 13.5, and 20. Urata et al.[11] found this distance increasing from 4.6 Å at $\lambda = 2.8$−7.7 Å at $\lambda = 35.4$ in their united-atom simulation. Thus, our simulations reveal that the sulfonate groups move away from each other with increasing membrane hydration in qualitative agreement with the findings of previous simulations.[9,11,15] The calculation of this sulfur−sulfur distance for different levels of membrane hydration in the present work establishes a classical benchmark for sulfonate−sulfonate separation in hydrated Nafion.

Figure 4b shows that the changes in $g_{Oh-Oh}(r)$ with increasing λ are similar to the changes in $g_{S-S}(r)$, especially at low hydration levels. This suggests that hydronium ions may be strongly bound to sulfonate groups at low λ consistent with the distribution of hydronium ions seen in Figure 3a. The area under $g_{Oh-Oh}(r)$ decreases with increasing λ indicating that the coordination number of hydronium oxygen atoms around each other, $n_{Oh-Oh}(r)$, decreases. The average distance from a hydronium ion within which another hydronium ion can be found ($n_{Oh-Oh}(r) = 1$) is 5.6, 5.9, 6.1, 6.4, 6.6, 6.8, 7.1, and 7.6 Å, respectively, at $\lambda = 1$, 3, 5, 7, 9, 11, 13.5, and 20. With increasing membrane hydration, the hydronium ions move away from each other just as the sulfonate groups move apart.

Panels c and d of Figure 4 represent the sulfonate−hydronium interaction in the form of $g_{S-Oh}(r)$ and $g_{Os-Oh}(r)$, respectively. For all values of λ, $g_{S-Oh}(r)$ shows a dominant peak between 3.85 and 3.92 Å. In contrast, the united-atom simulations of Cui et al.[14] give the first peak at 4 Å for the four λ values they examined. In our work, there is an additional peak at 3.2 Å only for $\lambda = 1$, which represents the contact ion pair (closest approach of H_3O^+ and SO_3^-). When water molecules are included, this peak disappears as water molecules pull the H_3O^+ away from the SO_3^-. When λ increases from 1 to 7, the area under the curve up to 4.3 Å (first hydration shell) decreases drastically, while the area under the next peak increases. This shows that as λ increases, H_3O^+ moves away from the first hydration shell of the sulfonate group and in to the second shell extending from 4.3 to 6.8 Å. This is confirmed by the plot of $g_{Os-Oh}(r)$ in Figure 4d. A sharp first peak occurs at a sulfonate oxygen-hydronium oxygen separation of ~2.5 Å (contact ion pair) and a broader second peak is at ~4.8 Å. The area under

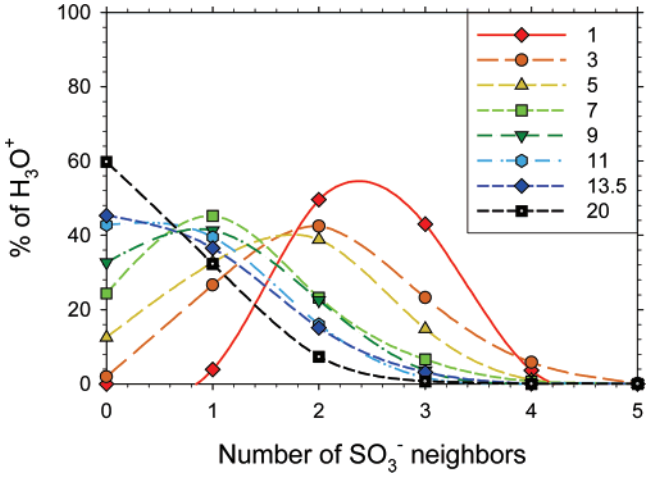

Figure 5. Distribution of sulfonate neighbors of hydronium ions in Nafion for various hydration levels, λ, indicated by the legend.

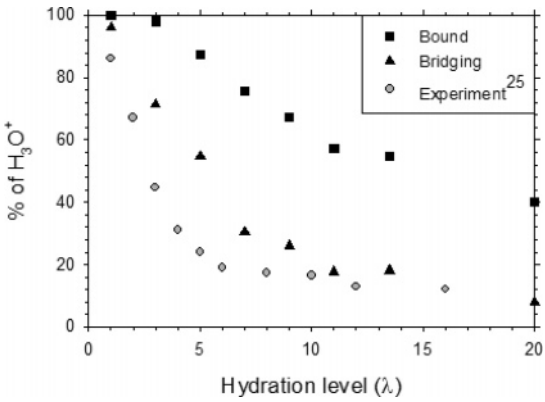

Figure 6. Percentages of hydronium ions that have at least 1 sulfonate neighbor (square) and multiple sulfonate neighbors (triangle) as a function of hydration level, λ, The percentage of nondiffusing hydrogen atoms obtained from neutron scattering experiment[25] is represented by circles.

these first two peaks decreases with increasing λ, while the area under the curve for the third neighbor shell located between ~5.2 and 7.2 Å increases with increasing λ. This indicates increasing separation with increasing λ. In agreement with Cui et al.,[14] we do not observe an "apparently artificial peak" at 3.2 Å that Petersen et al.[17] observed in their $g_{Os-Oh}(r)$ from classical simulations, which they attributed to the limitations of the classical hydronium ion. While the classical hydronium ion model does not incorporate proton shuttling (see ref 21), its limitations may have been overstated in the literature. Our simulations show that the hydronium ion can move away from the sulfonate group without the use of potentials that allow proton transfer.

The second peak in $g_{Os-Oh}(r)$ has been attributed by Cui et al.[14] to the sulfonate group and hydronium ion being separated by a layer of water molecules. This is true for large values of λ as we will show later in our discussion. However, our simulations show that the second peak occurs even when there are only hydronium ions and no water molecules present in the system ($\lambda = 1$). Therefore, at small values of λ, this peak can be attributed to multiple hydronium ions being present near each sulfonate group as a result of the sulfonate groups being close to each other. Evidence of this can be found by visual examination of the bottom right corner of Figure 3a. Further evidence in the form of the average number of hydronium oxygens within 4.3 Å of sulfur atoms (first hydration shell cutoff chosen based on $g_{S-Oh}(r)$) from 10 000 configurations is listed

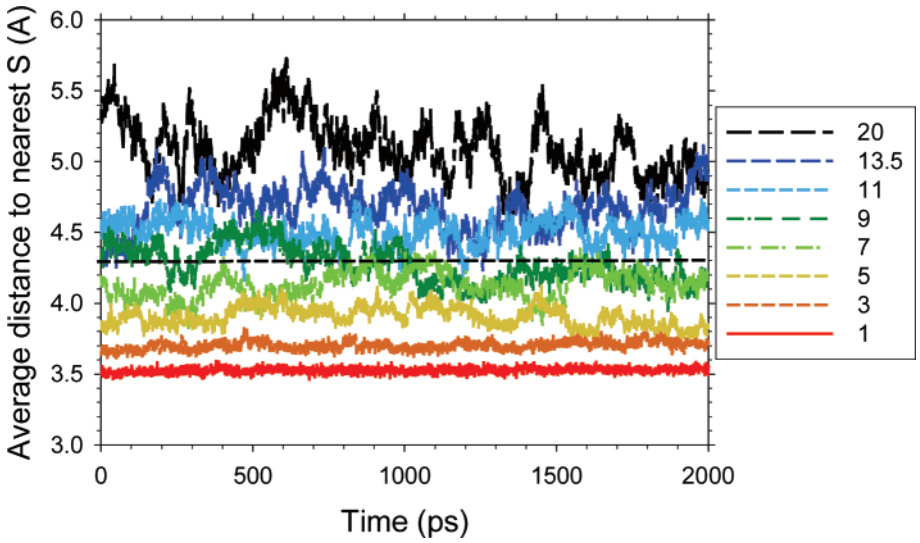

Figure 7. The average separation between hydronium oxygen and its nearest sulfur as a function of time for various hydration levels, λ, indicated by the legend.

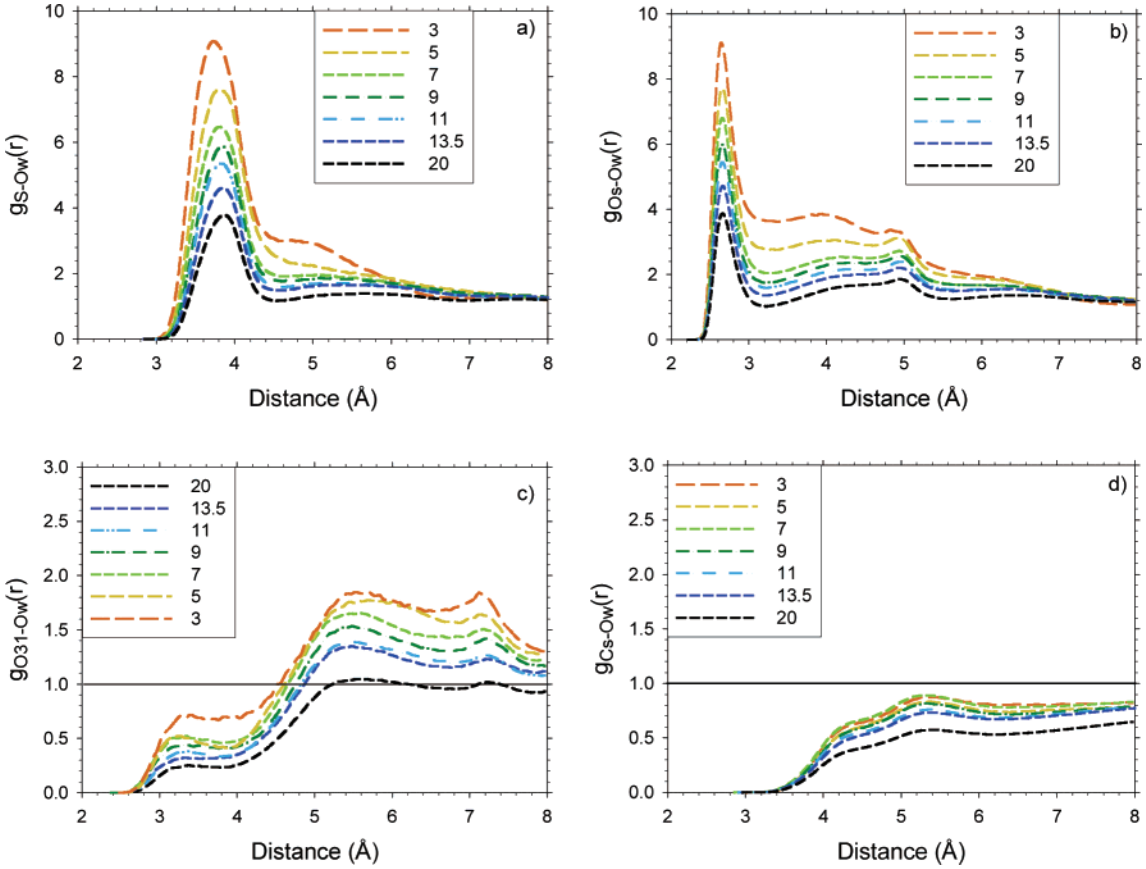

Figure 8. Radial distribution functions at various hydration levels (λ indicated by the legend) of water oxygen and (a) sulfur, (b) sulfonate oxygen, (c) first ether oxygen, and (d) backbone carbon.

in the second column of Table 3. This coordination number decreases rapidly from 2.46 at $\lambda = 1-1.14$ at $\lambda = 7$, starts to level off and reaches 0.49 at $\lambda = 20$. These results show that multiple hydronium ions are present around sulfonate groups at low levels of membrane hydration and that on average the hydronium ion moves away from the sulfonate group as λ increases.

Figure 5 shows the percentage of H_3O^+ with various numbers of SO_3^- groups within 4.3 Å in hydrated Nafion obtained from 2000 configurations at an interval of 1 ps. Lines have been drawn through the data points to guide the eye. For $\lambda = 1$, most of the hydronium ions have two or three SO_3^- neighbors. For $\lambda = 3$ or 5, the most likely configuration is a H_3O^+ with two SO_3^- neighbors, while for $\lambda = 7$ or 9, H_3O^+ is most likely to be coordinated with just one SO_3^- neighbor. Finally for $\lambda =$ 11 or higher, the most likely SO_3^- coordination number of H_3O^+ is zero (free hydronium ion). These results also show that even at the highest level of membrane hydration examined ($\lambda = 20$), some of the H_3O^+ are bound (have at least one SO_3^- neighbor). Of these bound H_3O^+, a significant percentage appears to form bridges between SO_3^- groups (coordinated by multiple SO_3^-). A bridging hydronium ion is less likely to become free and

take part in proton transport than a hydronium ion bound to only one sulfonate group.

Figure 6 is a plot of the percentage of H_3O^+ that are bound (squares) and those in bridging configurations (triangles) as a function of λ averaged from 2000 configurations at an interval of 1 ps. The percentage of bound H_3O^+ (with one or more SO_3^- neighbors) decreases almost linearly from 98% at $\lambda = 1-57\%$ at $\lambda = 11$ and then levels off to 40% at $\lambda = 20$. The percentage of bridging H_3O^+ decreases rapidly with increasing λ from 96% at $\lambda = 1$ to 30% at $\lambda = 7$ and then level offs to 18% at $\lambda = 13.5$ and finally reaches 8% at $\lambda = 20$. The fraction of bound H_3O^+that form bridges decreases with increasing λ from 0.96 at $\lambda = 1-0.20$ at $\lambda = 20$. Thus, one of the most notable effects of increasing the level of hydration of Nafion membrane is a significant decrease in the formation of $SO_3^- - H_3O^+ - SO_3^-$ bridges. The variation of the percentage of bridging H_3O^+ with membrane hydration shows excellent agreement with the variation of the percentage of non-diffusing hydrogen atoms determined by Pivovar and Pivovar[25] using quasi-elastic neutron scattering from Nafion 117 (circles).

Since the fraction of free H_3O^+ increases with increasing λ, it is important to examine the separation of H_3O^+ from its nearest SO_3^- as a function of λ. Figure 7 shows a plot of the distance separating the oxygen of H_3O^+ from its nearest sulfur atom averaged over the 40 H_3O^+ in the system. This data is plotted versus time at intervals of 1 ps (2000 data points for each value of λ). A horizontal dashed line is shown at a distance of 4.3 Å to represent the first neighbor cut off distance. For $\lambda \leq 7$, the average distance to the nearest SO_3^- remains within the first hydration shell radius for the entire duration of the simulation. For $\lambda > 9$, the average $H_3O^+ - SO_3^-$ separation remains beyond the first hydration shell radius for the entire duration of the simulation. The average $H_3O^+ - SO_3^-$ distance and the fluctuations in the data increase with increasing λ. The increased fluctuations in the data reflect the increased mobility of the hydronium ion.

3.3. Hydration of the Side Chain and Backbone. Panels a and b of Figure 8 represent the sulfonate-water interactions in the form of $g_{S-Ow}(r)$ and $g_{Os-Ow}(r)$, respectively. With increasing λ, the first peak in $g_{S-Ow}(r)$ decreases in height and its position moves to longer distances from 3.7 Å for $\lambda = 3$ to 3.85 Å for $\lambda = 20$. The peak height and positions are in excellent agreement with the results of Jang et al.[12] for $\lambda = 16$. However, this observation is in sharp contrast to the united-atom simulation results of Cui et al.[14] that showed a first peak at 4 Å for all values of λ. The plot of $g_{Os-Ow}(r)$ in Figure 8b shows a first peak at 2.65 Å for all values of λ and the height of this peak decreases with increasing λ. With an increase in the value of λ from 1 to 20, the number of H_3O^+ and SO_3^- remain the same at forty each, but the number of water molecules increases from 0 to 760. Thus, one cannot make inferences about the coordination number from the area under the $g_{S-Ow}(r)$ and $g_{Os-Ow}(r)$ curves unlike the case of $g_{S-Oh}(r)$ and $g_{Os-Oh}(r)$. The average number of water oxygens within 4.3 Å of sulfur atoms (first hydration shell) from 10000 configurations is listed in the third column of Table 3. Not surprisingly, the number of water molecules around the sulfonate group increases as λ increases, which is also evident in the sequence of projections in Figure 3. However, the increase in coordination number is not linear with λ, but instead increases rapidly till $\lambda = 5$ and saturates above $\lambda = 9$. The increased solvation of the sulfonate group results in water molecules mediating the hydronium ion-sulfonate group interaction and increasing the separation between H_3O^+ and SO_3^-. In addition to studying the local

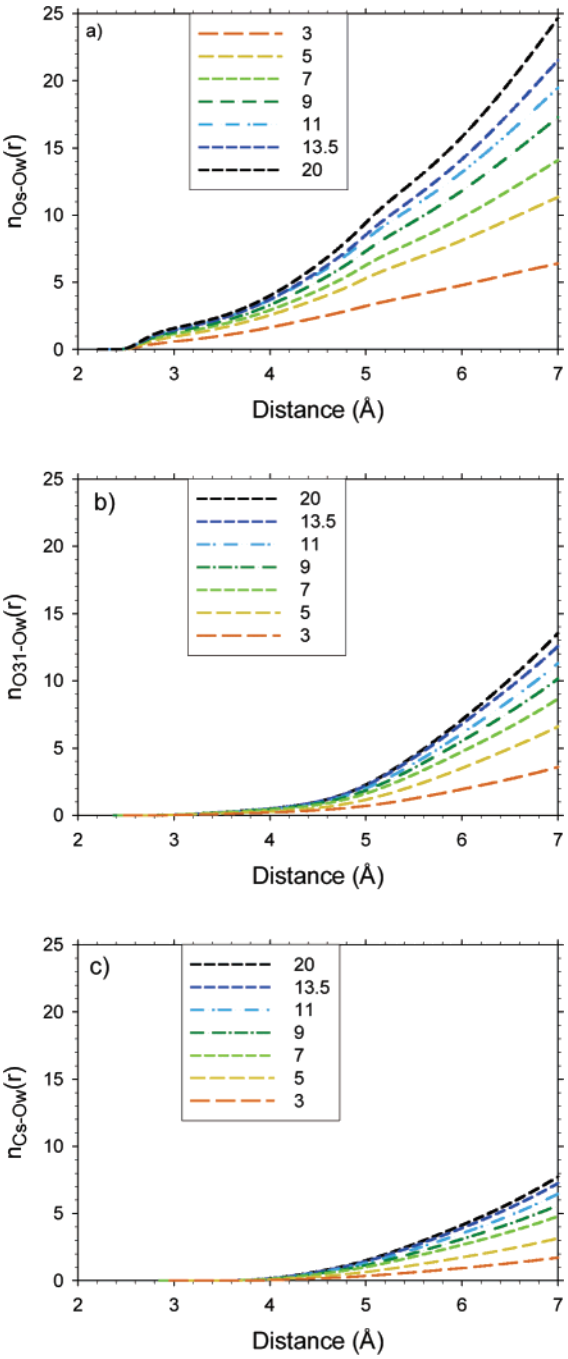

Figure 9. Hydration numbers (for λ values indicated by the legend) for (a) sulfonate oxygen, (b) first ether oxygen, and (c) backbone carbon atom.

structure around the sulfonate group, we have also examined the distribution of water molecules around the side chain and backbone of Nafion. Panels c and d of Figure 8 show plots of the RDF between water oxygen and ether oxygen closest to the sulfonate group, $g_{O31-Ow}(r)$, and backbone carbon, $g_{Cs-Ow}(r)$, respectively. The local number density of water molecules within 4.5−5 Å of the first ether oxygen and within 8 Å of the backbone carbon remains below the average number density of water molecules in the simulation cell, i.e., $g(r) < 1$ (horizontal line), which shows the hydrophobic nature of the ether oxygen and backbone carbon.

Further information about the presence of water molecules in the vicinity of the sulfonate group, the rest of the side chain and the backbone can be obtained by plotting the average number of water molecules (from 10 000 configurations)

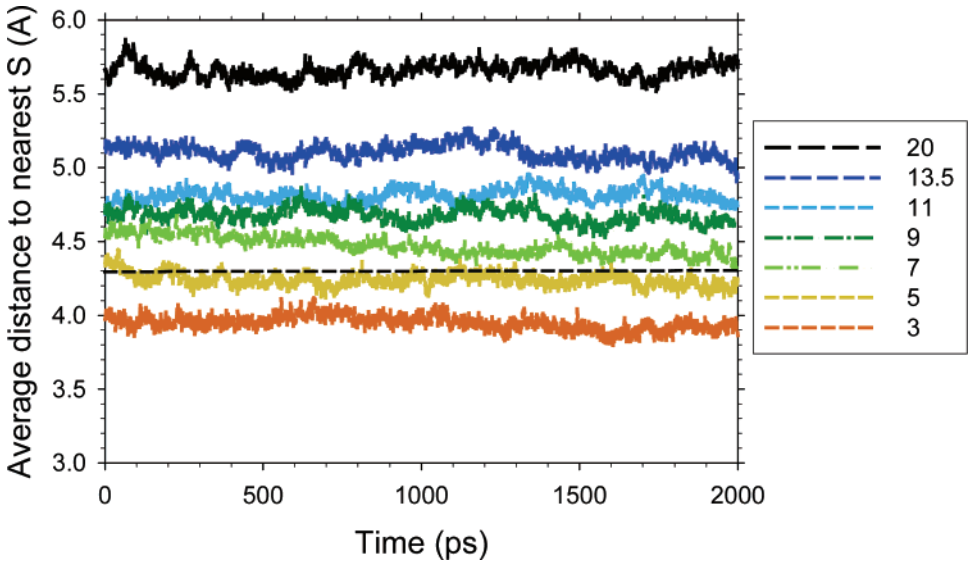

Figure 10. The average separation between water oxygen and its nearest sulfur as a function of time for various hydration levels, λ, indicated by the legend.

contained within a shell of a certain radius from various atoms as a function of λ. Figure 9 shows such a plot of water coordination number against radial distance around (a) sulfonate oxygen, (b) the ether oxygen closest to the sulfonate group, and (c) backbone carbon atom. Even at $\lambda = 20$, for a radius of 4.3 Å (cut off distance corresponding to the first minimum in $g_{S-Ow}(r)$), very few water molecules are present around the first ether oxygen and even fewer around the backbone carbon atoms. Thus, our results reveal the nanoscale separation of the hydrated Nafion membrane into hydrophilic and hydrophobic regions. As discussed by Vishnyakov and Neimark[10] and Urata et al.,[11] the hydrophilic subphase is just the sulfonate group at the end of the pendant. The ether oxygen that is closest to the sulfonate group is hydrophobic. The changes in hydration number with increasing λ in Figure 9c counter the inference from a recent infrared spectroscopy experiment[26] that the number of embedded water molecules in close proximity to the fluorocarbon is dramatically reduced for $\lambda \geq 5$. Our simulations clearly show that at all levels of membrane hydration, very few water molecules are in close proximity to the fluorocarbon part of the membrane and the hydration number increases with increasing λ. Some other explanation is needed to account for the changes in the structure and properties of Nafion brought about by changes in λ. By systematically calculating hydration numbers versus distance around various functional groups for a large number of values of λ, our work has quantified the nanophase separation in Nafion over a wide range of membrane conditions from dry to flooded membrane.

Figure 10 shows the average distance separating oxygen of H_2O from its nearest SO_3^- as a function of time for various λ. The horizontal dashed line shown at a distance of 4.3 Å represents the first neighbor cut off. The average water molecule is likely to remain bound only for $\lambda = 3$. For $\lambda > 5$, the average water molecule remains outside the first hydration shell of the nearest sulfonate group. The fluctuations in Figure 10 are smaller than those in Figure 7 due to averaging over a larger number of molecules (80 to 760 H_2O vs 40 H_3O^+). For all values of λ, the average distance from the nearest sulfonate group is shorter for H_3O^+ than for H_2O, which shows that the interaction of H_3O^+ with SO_3^- is stronger than that of H_2O with SO_3^-.

3.4. Hydronium Ions and Water Molecules. Figure 11 shows the RDF between oxygen of water molecule and (a) oxygen of hydronium ion and (b) oxygen of water molecule

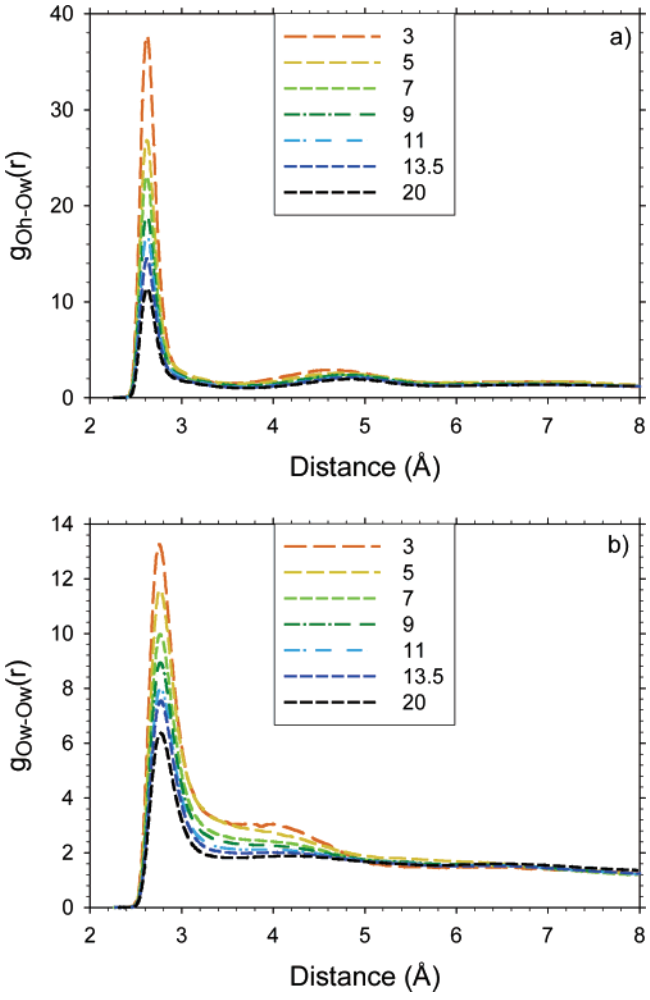

Figure 11. Radial distribution functions at various hydration levels (λ indicated by the legend) of water oxygen and (a) hydronium oxygen and (b) water oxygen pairs.

for various values of λ. The first peak in $g_{Oh-Ow}(r)$ occurs at 2.6 Å and the second peak is between 4.5 and 4.7 Å. $g_{Ow-Ow}(r)$ has a first peak between 2.7 and 2.8 Å. With increasing hydration level, the features exhibited by $g_{Ow-Ow}(r)$ in Nafion resemble those shown by bulk water as seen in Figure 2a. The

TABLE 4: The Average Coordination Numbers of Water Molecules around a Hydronium Ion (n_{hw}) and Water Molecules around a Water Molecule (n_{ww}) in Nafion as a Function of λ

λ	n_{hw}	n_{ww}
1	0.00	0.00
3	1.49	1.01
5	2.26	1.80
7	2.73	2.18
9	3.08	2.53
11	3.37	2.75
13.5	3.40	2.98
20	3.83	3.43

general features of these RDFs are similar to those previously observed in united-atom[11,14] and all-atom[15] force field simulations of Nafion. Based on Figure 11, we have chosen 3.3 Å as the first neighbor cutoff distance between oxygen of H_2O and oxygen of H_2O as well as oxygen of H_3O^+ for the calculation of hydration number.

Table 4 lists the number of water molecules in the first hydration shell of H_3O^+ and H_2O for various λ. For $\lambda < 9$, the average hydration number of H_3O^+ is less than 3. Cui et al.[14] have argued that structural transport of protons can be impeded if Eigen ions are not allowed to form. This requires at least three water molecules around a hydronium ion. The hydration number of H_3O^+ starts to saturate at about $\lambda = 11$, which is remarkably similar to the changes in nonbridging H_3O^+ (100%, bridging H_3O^+ %) in Figure 6. From the above results, it is clear that with increasing membrane hydration, more water molecules mediate the hydronium ion−sulfonate group interaction, which leads to increased separation between H_3O^+ and SO_3^- and formation of fewer H_3O^+ bridges between different SO_3^- groups.

Figure 12 is a plot of the percentage of hydronium ions with 1, 2, 3, 4, 5, and 6 water molecules within the first hydration shell for various λ obtained from 2000 configurations at an interval of 1 ps. Lines are drawn through the data points to guide the eye. At $\lambda = 3$ and 5, the most likely hydration number is 2 and Eigen ions are unlikely to form. The effect of increasing λ is to shift the curve to higher hydration numbers. Our simulation results suggest that the abrupt structural change in Nafion membrane above $\lambda = 5$ inferred from experiment,[26] is probably related to the changes in hydration number and bridging configurations of H_3O^+. These are related phenomena and represent the most prominent structural changes observed in our work.

In addition to increasing hydration number of H_3O^+, the number of water molecules in the first hydration shell of H_2O increase from ~1 for $\lambda = 3$ and approach bulk water-like values for $\lambda = 20$ as shown in Table 4. Figure 12 is a plot of the relative percentage of water molecules bound to SO_3^-, weakly bound water molecules and free water molecules as a function of λ. The data was obtained as an average over 2000 configurations at each λ. First, we classified all the water molecules whose oxygen atom was within 4.3 Å of a sulfur atom as bound water molecules. Then, we classified the remaining water molecules whose oxygen atom had four other water oxygen neighbors within 4 Å as free water molecules based on our simulation of bulk water discussed earlier. Finally, we classified the remaining water molecules as weakly bound water molecules. As λ increases, the percentage of free water increases monotonically from 2.7% for $\lambda = 3$ to 66% for $\lambda = 20$. The percentage of bound water decreases from ~82% for $\lambda = 3$ to 28% for $\lambda = 20$. The percentage of weakly bound water also decreases monotonically with an increase in λ.

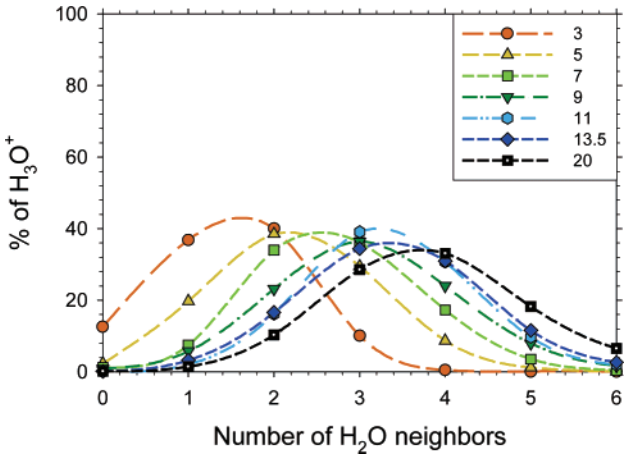

Figure 12. The distribution of water around hydronium ions in Nafion for various hydration levels, λ, indicated by the legend.

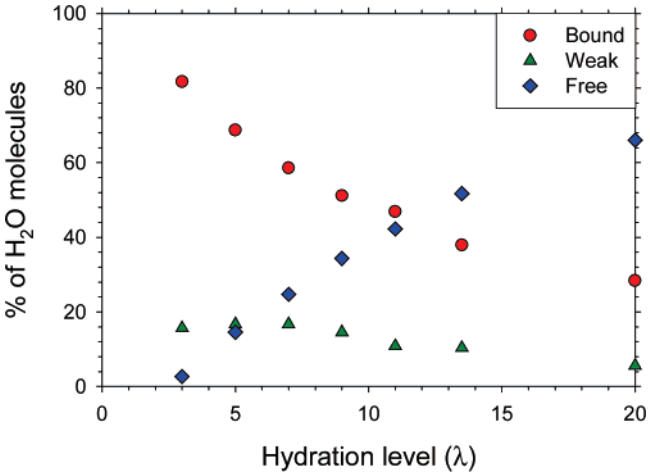

Figure 13. The relative proportions of bound, weakly bound, and free water molecules in Nafion as a function of hydration level, λ.

The present work has provided insights into nanoscale phase separation in hydrated Nafion and provided an explanation for the changes observed experimentally with increasing hydration level. By systematically varying λ from 1 to 20 and making direct comparison to experimental observations of non diffusing hydrogen atoms, we have highlighted the dominant role of H_3O^+ bridges in impeding proton transport. For $\lambda \leq 7$, hydronium ions are surrounded by multiple sulfonate groups. As shown in Figure 7, binding to multiple sulfonate groups prevents the hydronium ion from becoming free and contributing to vehicular proton transport. At the same time, steric hindrance from the sulfonate groups, impedes hydration of H_3O^+. This prevents structural transport of protons. We will discuss the relationship between the structural changes described here and changes in dynamical properties in the second part of this report.

4. Conclusions

We have simulated the effect of hydration on Nafion membrane nanostructure at different degrees of membrane hydration using classical molecular dynamics simulations with the DREIDING force field. We found that increasing membrane hydration causes the sulfonate groups to move apart. At λ less than 7, most of the water molecules and hydronium ions are bound to the sulfonate groups. The strong binding of hydronium ions to sulfonate groups prevents vehicular transport of protons. In addition, multiple sulfonate groups surrounding the hydronium ion (bridging configuration of H_3O^+) at low hydration

offer steric hindrance to hydration of the hydronium ion, which hinders structural diffusion of protons. This conclusion is supported by the variation with λ of the fraction of hydronium ions that are in bridging configurations being in excellent agreement with the variation of non-diffusing hydrogen atoms determined by neutron scattering experiments. Water molecules are mainly found in the vicinity of the sulfonate groups, while the ether oxygen and backbone are strongly hydrophobic. Our results provide atomic-level insights into structural changes observed in Nafion by infrared spectroscopy.

Acknowledgment. This work was supported by the U.S. Department of Energy's (DOE) Office of Basic Energy Sciences, Chemical Sciences Program, and was performed in part using the Molecular Science Computing Facility (MSCF) in the William R. Wiley Environmental Molecular Sciences Laboratory, a DOE national scientific user facility located at the Pacific Northwest National Laboratory (PNNL). PNNL is operated by Battelle for DOE. This work benefited from resources of the National Energy Research Scientific Computing Center, which is supported by the Office of Science of the U.S. Department of Energy under Contract No. DE-AC03-76SF00098.

References and Notes

(1) Crabtree, G. W.; Dresselhaus, M. S.; Buchanan, M. V. *Phys. Today* **2004**, *59* (12), 39.
(2) Kreuer, K.-D.; Paddison, S. J.; Spohr, E.; Schuster, M. *Chem. Rev.* **2004**, *104*, 4637.
(3) Mauritz, K. A.; Moore, R. B. *Chem. Rev.* **2004**, *104*, 4535.
(4) Hickner, M. A.; Ghassemi, H.; Kim, Y. S.; Einsla, B. R.; McGrath, J. E. *Chem. Rev.* **2004**, *104*, 4587.
(5) Steele, B. C. H.; Heinzel, A. *Nature* **2001**, *414*, 345.
(6) Eikerling, M; Kornyshev, A. A.; Kucernak, A. R. *Phys. Today* **2006**, *59* (10), 38.
(7) Paddison, S. J. *Annu. Rev. Mater. Res.* **2003**, *33*, 289.
(8) Paddison, S. J.; Elliott, J. A. *J. Phys. Chem. A* **2005**, *109*, 7583.
(9) Elliott, J. A.; Hanna, S.; Elliott, A. M. S.; Cooley, G. E. *Phys. Chem. Chem. Phys.* **1999**, *1*, 4855.
(10) Vishnyakov, A.; Neimark, A. V. *J. Phys. Chem. B* **2001**, *105*, 9586.
(11) Urata, S.; Irisawa, J.; Takada, A.; Shinoda, W.; Tsuzuki, S.; Mikami, M. *J. Phys. Chem. B* **2005**, *109*, 4269.
(12) Jang, S. S.; Molinero, V.; Çа_gun, T.; Goddard, W. A. *J. Phys. Chem. B* **2004**, *108*, 3149.
(13) Blake, N. P.; Mills, G.; Metiu, H. *J. Phys. Chem. B* [Early online access.] DOI: 10.1021/jp066473v.
(14) Cui, S.; Liu, J.; Selvan, M. E.; Keffer, D. J.; Steele, W. V. *J. Phys. Chem. B* [Early online access.] DOI: 10.1021/jp066388n.
(15) Venkatnathan, A.; Devanathan, R.; Dupuis, M. *J. Phys. Chem. B* **2007**, *111*, 7234.
(16) Spohr, E. *Mol. Simul*. **2004**, *30*, 107.
(17) Petersen, M. K.; Wang, F.; Blake, N. P.; Metiu, H.; Voth, G. A. *J. Phys. Chem. B* **2005**, *109*, 3727.
(18) Petersen, M. K.; Voth, G. A. *J. Phys. Chem. B* **2006**, *110*, 18594.
(19) Wescott, J. T.; Qi, Y.; Subramanian, L.; Capehart, T. W. *J. Phys. Chem. B* **2006**, *124*, 134702.
(20) Paul, R.; Paddison, S. J. *J. Chem. Phys.* **2005**, *123*, 224704.
(21) Marx, D. *Chem. Phys. Phys Chem* **2006**, *7*, 1848.
(22) Mayo, S. L.; Olafson, B. D.; Goddard, W. A. *J. Phys. Chem.* **1990**, *94*, 8897.
(23) Jang, S. S.; Blanco, M.; Goddard, W. A.; Caldwell, G.; Ross, R. B. *Macromolecules* **2003**, *36*, 5331.
(24) Levitt, M.; Hirshberg, M.; Sharon, R.; Laidig, K. E.; Daggett, V. *J. Phys. Chem. B* **1997**, *101*, 5051.
(25) Pivovar, A. M.; Pivovar, B. S. *J. Phys. Chem. B* **2005**, *109*, 785.
(26) Moilanen, D. E.; Piletic, I. R.; Fayer, M. D. *J. Phys. Chem. A* **2006**, *110*, 9084.
(27) Payne, M. C.; Teter, M. P.; Allan, D. C.; Arias, T. A.; Joannopoulos, J. D. *Rev. Mod. Phys*. **1992**, *64*, 1045.
(28) Morris, D. R.; Sun, X. *J. Appl. Polym. Sci.* **1993**, *50*, 1445.
(29) Todorov, I. T.; Smith, W.; Trachenko, K.; Dove, M. T. *J. Mater. Chem.* **2006**, *16*, 1911.
(30) Vishnyakov, A.; Neimark, A. V.; *J. Phys. Chem. B* **2001**, *105*, 7830.
(31) Essmann, U.; Perera, L.; Berkowitz, M. L.; Darden, T.; Lee, H.; and Pedersen, L. G. *J. Chem. Phys.* **1995**, *103*, 8577.
(32) Soper, A. K.; Phillips, M. G. *Chem. Phys*. **1986**, *107*, 47−60.
(33) Humphrey, W.; Dalke, A.; Schulten, K. *J. Mol. Graphics* **1996**, *14*, 33.